25th ABCM International Congress of Mechanical Engineering
October 20-25, 2019, Uberlândia, MG, Brazil

COB-2019-0719
NUMERICAL STUDY OF THE VISCOSITY INFLUENCE ON VERTICAL ASCENDANT LIQUID-GAS FLOW IN A DISTRIBUTOR

Juan P. F. Albuquerque
Carolina C. Rodrigues
Henrique K. Eidt
Dalton Bertoldi
Paulo H. D. Santos
Rigoberto E. M. Morales
Multiphase Flow Center (NUEM), Federal University of Technology – Paraná (UTFPR) – Rua Deputado Heitor Alencar Furtado 5000, Bloco N, CEP 81280-340, Curitiba, Brazil.
albuquerque@alunos.utfpr.edu.br, carolcimarelli@gmail.com, hkeidt@gmail.com, daltonbertoldi@utfpr.edu.br, psantos@utfpr.edu.br, rmorales@utfpr.edu.br

Abstract. *Multiphase flow occurs frequently in the production of offshore petroleum and can cause several problems such as intermittent flow, hydrate deposition, and severe slugging. These issues can be prevented by use of separators. However, due to their large dimensions, they use in the seabed is avoided. An alternative to reduce their sizes is to install a distribution system, whereas more than one separator can be used. The purpose of the present work is to analyze numerically the effects of viscosity in the behavior of ascendant liquid-gas swirling flow in the distribution system of a vertical separator. CFD simulations of a three-dimensional hybrid mesh were carried out at the commercial software ANSYS-CFX 2019. Numerical simulations were based on a finite volume method based on finite element with Eulerian-Eulerian two fluid and Shear Stress Transport (SST) turbulence models. A compressive discretization scheme was used to capture the liquid-gas interface. Mass flow rates at the outlets of the system were evaluated in order to estimate the distribution capacity. The results showed that the centrifugal forces in a cyclonic chamber decrease with increasing viscosity. However, system distribution capacity was not influenced by liquid viscosity.*

Keywords: *CFD, numerical analysis, distribution system, vertical ascendant liquid-gas flow, viscosity.*

1. INTRODUCTION

In the petroleum industry, multiphase flow occurs during the production and transportation of petroleum. According to Rodrigues *et al*. (2017), multiphase flow can be simplified as a two-phase flow, in which a mixture of oil and water is the liquid phase, and the gas is the other phase itself. The presence of more than one phase impairs the operation of equipment, such as compressors and pumps, originally designed for single-phase flows. In these situations, it is recommended to separate the phases at the wellhead level. The separation process on the seabed has several advantages, such as avoiding or reducing typical problems of multiphase flows (intermittent flow, hydrate deposition, severe slugging) as well as increasing the efficiency of submersible centrifugal pumps (Eidt *et al*., 2017a). To improve this process, a separation system is employed, such as VASPS (Vertical Annular Separation and Pumping System) or GLCC (Gas-Liquid Cylindrical Cyclone). Although these separators increase the efficiency of separation, they have large dimensions, which hamper the construction, installation, and maintenance of them in offshore applications.

With the aim of reducing these dimensions, studies were performed to develop a distribution system that can divide the liquid and gas flows into more separators, with smaller dimensions and without affecting the separation efficiency or decreasing oil production (Eidt *et al*., 2017b). This distribution system consists of one inlet, a cyclonic chamber, and four outlets, and is shown in Figure 1 with dimensions used in the numerical study. In the cyclone chamber, the flow enters through two nozzles tangentially oriented, which combined with cyclonic chamber curvature leads to the generation of a centrifugal field, forming a swirling flow. This flow has the characteristic in which a thin liquid film flows near the wall, while the gas flows in the region of axial core (Gupta *et al.*, 1984).

In an experimental study developed by Shakutsui et al. (2000) it was observed that for the vertical ascendant flow, the centrifugal field undergoes the greater influence of the liquid phase which was also observed by Eidt (2017). Liu and Bai (2014) have observed that the centrifugal field intensity decrease with the swirl flow development, and that each case has a swirl length after which the flow returns to the previous pattern. Besides that, it is known that the viscosity increasing will influence this formed liquid film. Rosa *et al*. (2001) noted that the increase in liquid phase

viscosity implies a reduction in the separation capacity of the cyclonic separator studied. Brito and Trujillo (2009) associated the increase of viscosity with the reducing of separation capacity of these systems. Rodrigues *et al*. (2017) concluded that as the viscosity increases, the centrifugal force decreases, which causes the stability of the film to be impaired.

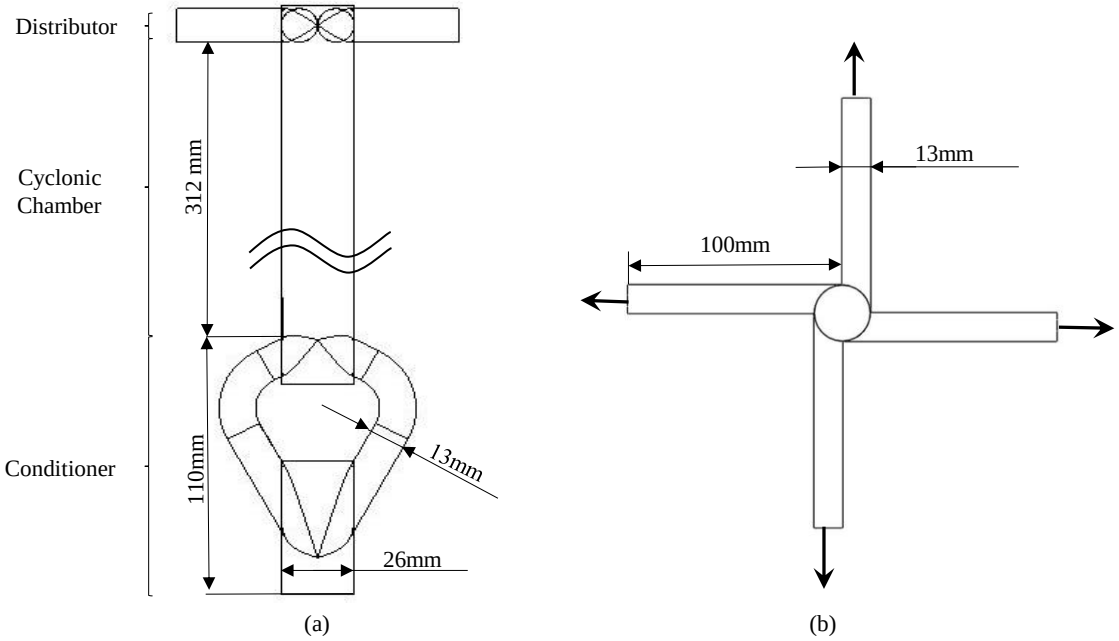

Figure 1. Schematic scheme of distribution system parts and dimensions: (a) side view; (b) top view.

The goal of this study was to analyze the effects of the viscosity in the behavior of the average liquid film thickness inside the cyclonic chamber and the distribution capacity considering the liquid-gas mass flow rate on outlets.

2. NUMERICAL MODEL

The phenomena were analyzed numerically through the resolution of the unsteady Reynolds-averaged Navier–Stokes equations, usually referred to as U-RANS equations, using the software ANSYS-CFX - 2019.

2.1 Mathematical modeling

The continuity and Navier-Stokes equations can be written as:

$$\frac{\partial \rho}{\partial t} + \nabla.\left(\rho \vec{V}\right) = 0 \tag{1}$$

$$\frac{\partial \rho \vec{V}}{\partial t} + \nabla \cdot (\rho \vec{V}\vec{V}) = -\nabla(p) + \nabla \cdot \left[\mu_{eff} \nabla \vec{V}\right] + \rho g + F_D \tag{2}$$

where ρ is the density, $\vec{V}$ is the Reynolds averaged velocity vector, p is the pressure, g is the gravity, μ_{eff} is the fluid dynamic efficient viscosity ($\mu_{eff} = \mu + \mu_T$, μ is the fluid dynamic viscosity and μ_T is the turbulent or eddy viscosity, a term that appears based on the Boussinesq hypothesis and has to be modeled) and F_D is the drag force per volume unit between phase.

The Eulerian-Eulerian model was used to solve the equations (1) and (2) for each phase. This model assumes an inertial frame of reference for the phases and considers these phases as inhomogeneous in the velocity field, interpenetrating and continuous (Eidt *et al.*, 2016). To model the turbulent viscosity was used the SST model (Shear Stress Transport), and it is considered a turbulence homogeneous field. The SST model is not based on wall functions and it is said to handle liquid-film flow generally better than other two-equation turbulence models (ANSYS, 2019). To characterize the interface between the phases is applied a compressive discretization scheme in order to reduce the diffuseness in the interface, which is characteristic of the Eulerian-Eulerian two-phase approach.

The distribution system boundary conditions are schematically shown in Figure 2. No-slip wall conditions were adopted. At the outlets were set a reference static pressure of 0 Pa. A turbulence intensity of 5% was utilized. Slug flow was set at the inlet and representative unit cells were generated for each case, using the model developed by Eidt (2017). The flow was considered three dimensional, transient, isothermal and incompressible. The initial condition considers the geometry fully filled with the gas phase, with velocity equals to zero.

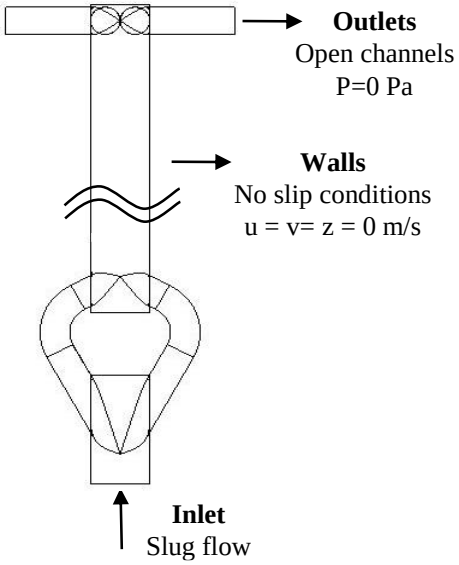

Figure 2. Schematic scheme of boundary conditions of the distribution system.

2.2 Computational mesh

Figure 3 shows the hybrid mesh used for the numerical model with tetrahedral volume elements at the conditioner and distributor regions, and hexahedral volume mesh at the cyclone chamber with mesh refinement near the wall, as required by the SST turbulence model (requires that dimensionless distance should be $y^+ < 2$). The total number of nodes of the selected grid is around 1,152,140. The time step and total time simulation used were 0.001 s and 2 s, respectively.

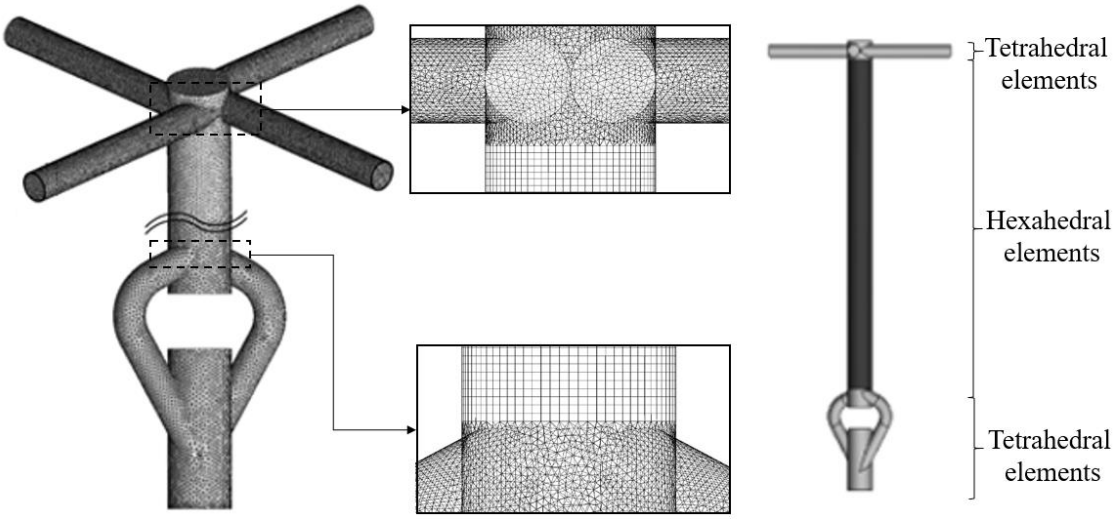

Figure 3. Computational mesh used.

The numerical simulations validation was performed with two different combinations of water and air surface velocities, using experimental data provided by Wire-mesh and ultrasonic sensors, which were obtained by Eidt (2017). Table 1 shows the difference between the numerical and experimental average liquid film thickness data.

Table 1. Comparison between numerical and experimental average liquid film data

j_L [m/s]	j_G [m/s]	Numerical δ[mm]	Wire-mesh sensor		Ultrasonic sensor	
			δ[mm]	Dif. [%]	δ[mm]	Dif. [%]
1.0	1.0	7.37	5.93	19.56	5.94	19.56
1.5	1.0	7.12	5.97	16.16	5.91	17.01

The maximum numerical deviation was 19.59% for the case with both superficial velocities equal 1.0 m/s. Since simplifications have been adopted in order to validate the numerical model, the results can be considered precise. Moreover, the experimental results may contain errors related to the lack of measurement equipment accuracy. Thus, the numerical results are reliable for the flow inside the cyclonic chamber understanding.

3. RESULTS AND DISCUSSIONS

Numerical simulations were performed for two-phase flow: the first fluid was air and second one was water, Mineral Oil Excel 15 or Mineral Oil Excel 22. The density, viscosity and surface tension of each liquid phase are shown in Table 2. The gas properties are 1.2 kg/m³ for density and 0.0181 cP for dynamic viscosity.

Table 2. Properties of fluids used

Fluid	*Density [kg/m³]*	*Viscosity [cP]*	*Surface tension [N/m]*
Water	997.0	1.0	0.07287
Mineral oil Excel 15	837.5	28.5	0.00624
Mineral oil Excel 22	841.8	42.6	0.00629

The inlet conditions are based on a step function, which is defined by the superficial velocity of air (j_G) and liquid phase (j_L). The superficial velocities of each case can be seen in Table 3.

Table 3. All the cases analyzed numerically

Liquid phase	j_L [m/s]	j_G [m/s]	j_L [m/s]	j_G [m/s]	j_L [m/s]	j_G [m/s]
Water	0.5	1.0	1.0	1.0	1.5	1.0
Mineral oil Excel 15	0.5	1.0	1.0	1.0	1.5	1.0
Mineral oil Excel 22	0.5	1.0	1.0	1.0	1.5	1.0

According to Eidt (2017), the liquid superficial velocity influence on the swirling flow is greater than the gas superficial velocity influence. Thus, the liquid superficial velocity variation is sufficient to observe the fluid effects on this flow, while maintaining the gas superficial velocity in 1.0 m/s.

With the aim of analyzing the flow behavior inside the cyclonic chamber, it was first evaluated the liquid film formation across all the cyclonic chamber. Thereunto, planes with a 5 mm spacing were created along the cyclonic chamber and, in these planes, were calculated the average liquid film thickness, $\bar{\delta}$, based on the average void fraction, as can be seen in equation 3. The results obtained are shown in Figure 4.

$$\bar{\delta} = R\left(1-\sqrt{\bar{\alpha}}\right) \tag{3}$$

where R is the radius of the cyclonic chamber and $\bar{\alpha}$ is the average void fraction in the analyzed cross-section.

Figure 4 shows the average liquid film for all the cases analyzed numerically. It is possible to observe that there is an increase in the thickness film as the liquid phase surface velocity is increased, since there is a greater amount of liquid flowing. It is also observed that for all the flows analyzed a film oscillation stabilization in the axial direction occurs starting from the 150 mm at cyclonic chamber. However, it was not possible to observe a film thickness behavior related to the increase of the viscosity, since in Figure 4 the curves have different oscillations.

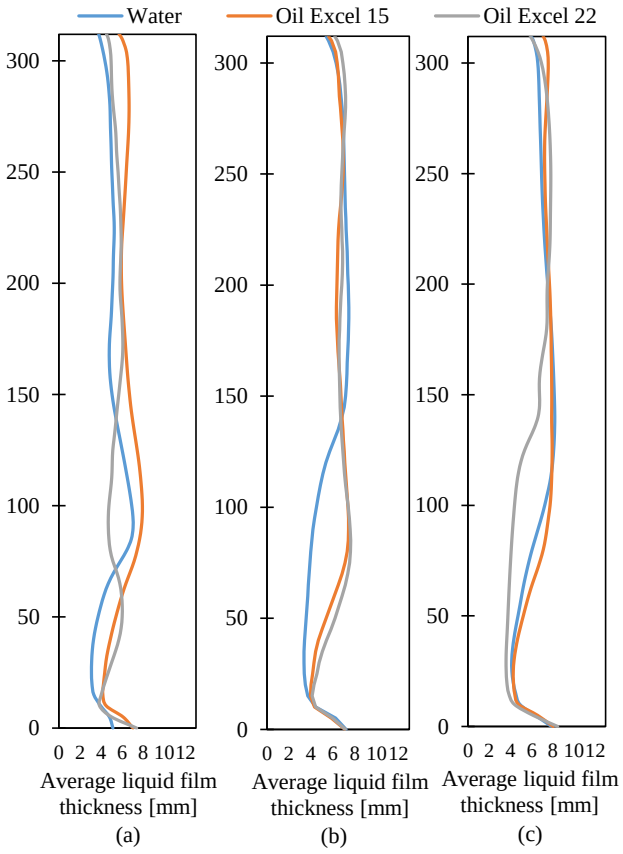

Figure 4. Average liquid film thickness along cyclonic chamber for (a) j_L=0.5 m/s (b) j_L=1.0 m/s (c) j_L=1.5 m/s.

To understand the variation in the flow behavior caused by the viscosity, the streamlines were evaluated on the cyclonic chamber for the cases described in Table 3. When analyzed the variation in the liquid superficial velocity for the same fluid, it was observed that the increase in liquid phase velocity causes the slope streamlines to decrease, owing the increase in liquid velocity implies a greater intensity in the swirling flow. Also, a comparison of the streamlines for the three different fluids, at the same superficial velocity, can be seen in Figure 5.

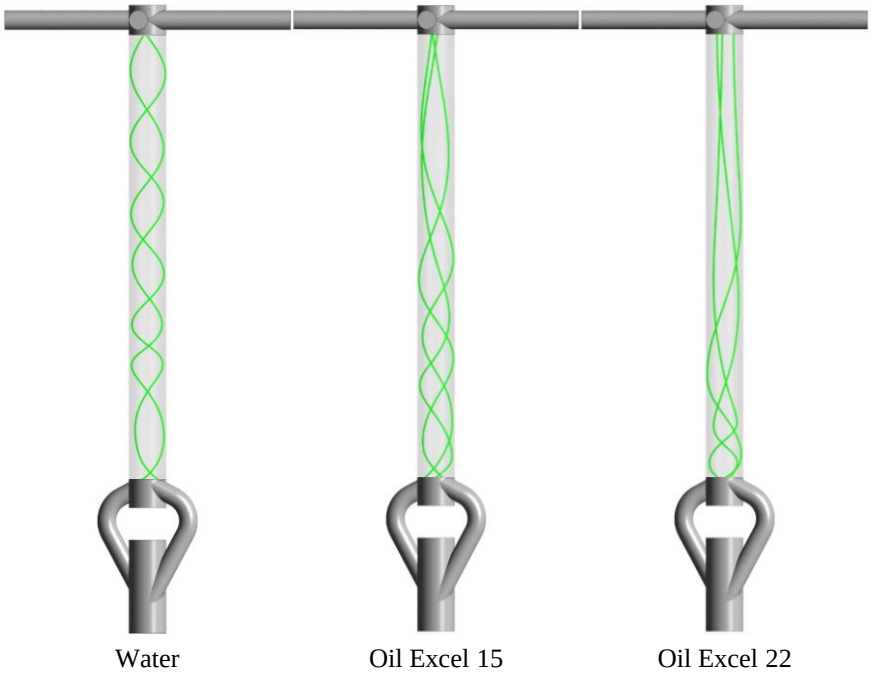

Figure 5. Streamlines for different fluids with j_L = 0.5 m/s.

Figure 5 indicates that the increase in liquid phase viscosity promotes a tangential force decrease along the flow, which can be observed by increasing the streamlines slopes along the cyclonic chamber. The intensity in the swirling flow decrease is caused by the increase of viscous dissipation in the cyclonic chamber, which is proportional to the liquid phase viscosity, using the same flow conditions. This means that increasing the liquid viscosity decreases the swirl length.

In order to evaluate the system distribution capacity, it was observed the average mass flow rate of the phases distribution at the outlets. Liquid volume fraction on the distribution system outlets for j_L=1.5 m/s and j_G =1.0 m/s is shown in Figure 6.

In Figure 6 it was observed that all analyzed liquid phases have a similar average distribution and behavior in their outlets. This performance was also noticed for the other combinations of superficial velocities. When comparing the liquid phases of different viscosities, it was noted that increasing the viscosity implies a smaller separation between the phases. In water-air flow (Figure 6-a) a better distinction can be seen between the liquid and gaseous phases. In mineral oil-air flow (Figure 6-b and Figure 6-c) the phases distinction was not observed, predominating a mixture between the two fluids. This is explained by the smaller tangential force present in the cyclonic chamber (Figure 5). The lower swirling flow intensity in the cyclonic chamber implies a lower phase pre-separation, which is clear in comparison shown in Figure 6.

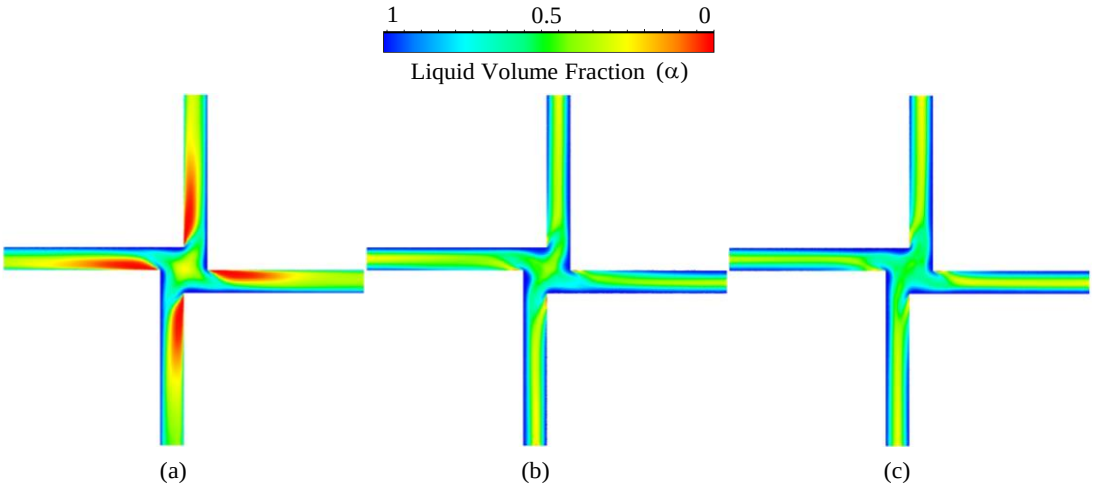

Figure 6. Average liquid volume fraction at the outlets for j_L =1.5 m/s and as the liquid phase: (a) Water (b) Oil Excel 15 (c) Oil Excel 22.

In order to clarify this described performance, Table 4 shows the percentages relative to the mass flow rate of liquid flowing at each outlet for all the cases analyzed numerically.

Table 4. Comparison between percentages relative to the four outlets in the mass flow rate of liquid.

Liquid phase	j_L [m/s]	j_G [m/s]	Outlet 1 [%]	Outlet 2 [%]	Outlet 3 [%]	Outlet 4 [%]
Water	0.5	1.0	24.99	24.34	25.30	25.37
	1.0	1.0	25.66	24.43	24.53	25.38
	1.5	1.0	26.37	24.22	24.17	25.24
Oil Excel 15	0.5	1.0	24.08	26.58	23.93	25.41
	1.0	1.0	24.57	25.15	25.20	25.07
	1.5	1.0	25.33	25.93	24.89	23.85
Oil Excel 22	0.5	1.0	24.01	25.20	26.80	23.99
	1.0	1.0	25.45	24.83	25.50	24.22
	1.5	1.0	25.78	24.17	25.43	24.61

The Table 4 results showed that the system distribution capacity was not dependent on the fluid viscosity and phase's superficial velocity, owing that in all cases the outlets reached approximately 25% of the liquid mass flow rate, which is the main goal. The maximum deviation is below 3 percent point in relation between the two worst outlets.

These results indicate that the system is capable to distribute liquid phases with viscosity up to 42 cP equally. Furthermore, no bond was observed between the system distribution capacity and the increase in liquid phase viscosity.

In the same way, Table 5 shows the percentages relative to the gas mass flow at each outlet for all the cases. The gas maximum deviation is below 4 percent point in relation between the two worst outlets. Thus, it indicates that this system is also able to distribute the gaseous phase, independent of liquid phase viscosity.

Table 5. Comparison between percentages relative to the four outlets in the mass flow rate of gas.

Liquid phase	j_L [m/s]	j_G [m/s]	Outlet1 [%]	Outlet2 [%]	Outlet3 [%]	Outlet4 [%]
Water	0.5	1.0	24.89	24.37	25.76	24.98
	1.0	1.0	25.42	24.75	24.62	25.21
	1.5	1.0	26.63	24.50	23.60	25.27
Oil Excel 15	0.5	1.0	23.79	27.24	23.47	25.20
	1.0	1.0	24.58	25.08	25.20	25.13
	1.5	1.0	25.48	26.14	24.79	23.59
Oil Excel 22	0.5	1.0	23.55	25.67	27.06	23.73
	1.0	1.0	25.78	24.63	26.03	23.56
	1.5	1.0	26.28	23.77	25.67	24.27

4. CONCLUSIONS

According to previous results, it could be concluded that the numerical model was capable of simulating the ascendant swirling two-phase flow (air and water/mineral oil) in the distribution system. The tubes tangentially positioned in the inlets of cyclonic chamber created a centrifugal field capable of forming a liquid film flow for all the cases analyzed numerically. In addition, it was observed that the increase in liquid phase viscosity leads to a decrease in the centrifugal force intensity along the cyclonic chamber. The centrifugal forces decrease promotes a smaller phase separation at the cyclonic chamber. However, the system distribution capacity was not altered by increasing liquid phase viscosity, presenting satisfactory distributions independent of the fluid viscosity, with the highest difference at 3 and 4 percent points for liquid and gas distribution, respectively. It is noteworthy that the variations in the behavior of the liquid-gas flow was attributed to the viscosity, even though the surface tension for the liquid phase were changed.

5. ACKNOWLEDGMENTS

The authors acknowledge the UTFPR, NUEM, and PETROBRAS for the infrastructure, support, and assistance for the development of this study.

6. REFERENCES

ANSYS, 2019. ANSYS® Academic Research, Release 14.5, Help System, CFX Documentation. ANSYS, Inc.

Brito, A. and Trujillo, J., 2009. "Viscosity effect in cylone separators" *Latin American and Caribbean Petroleum Engineering Conference*, Cartagena, Colombia.

Eidt, Henrique Krainer, 2017. "Analysis of the Ascendant Liquid Film Flow Development Under the Effect of Centrifugal and Gravitational Fields". *MSc Thesis - Postgraduate Program in Mechanical and Materials Engineering*, Federal University of Technology - Paraná, Curitiba, 130p.

Eidt, H.K., Rodrigues, C.C., Dunaiski, R., Ofuchi, C.Y., Neves Junior, F., Santos, P.H.D. and Morales, R.E.M., 2017. "Numerical and experimental analysys of vertical ascendant liquid-gas flow under action of centrifugal and gravitational fields". *Fluids Engineering Division Summer Meeting*, Waikoloa, Havaii, USA.

Eidt, H.K., Rodrigues, C.C., Dunaiski, R., Ofuchi, C.Y., Neves Junior, F., Santos, P.H.D. and Morales, R.E.M., 2017. "Experimental validation by ultrassonic technique of the numerical analysys of na ascendant flow under the influence of the centrifugal and gravitational fields". In *Proceedings of the 24nd International Congress of Mechanical Engineering - COBEM 2017*. Curitiba, Brazil.

Eidt, H.K., Rodrigues, C.C., Santos, P.H.D. and Morales, R.E.M., 2016. "Numerical analysys of a vertical ascendant two-phase flow in a cyclonic chamber under the action of centrifugal and gravitational fields". In *Proceedings of the 16nd Brazilian Congress of Thermal Sciences and Engineering - ENCIT 2016*. Vitória, Brazil.

Gupta, A. K., Lilley, D. G., & Syred, N., 1984. "Swirl flows". *Tunbridge Wells, Kent, England, Abacus Press, 1984, 488 p.*

Liu, W., Bai, B. F., 2014. “Two-phase flow patterns and pressure drop inside a vertical pipe containing a short helical tape insert”. *Fluids Engineering Division Summer Meeting*, Chicago, Illinois, USA

Rodrigues, C.C., Eidt, H.K., Dunaiski, R., Ofuchi, C.Y., Neves Junior, F., Santos, P.H.D. and Morales, R.E.M., 2017. “Numerical study of transient flow and the influence of height and viscosity in a ciclonic chamber in a distribution system”. *Fluids Engineering Division Summer Meeting*, Waikoloa, Havaii, USA.

Rosa, E., França, F. and Ribeiro, G., 2001. “The cyclone gas-liquid Separator: Operation and mechanistic modeling”. *Journal of Petroleum Science and Engineering*, Brazil.

Shakutsui, H., Watanabe, K., Onari, H., Saga, T., Kadowaki, H., 2000. “Flow patterns in swirl gas-liquid two-phase flow in a vertical pipe”. In *Proceedings of the 4th Thermal Engineering Conference.* Kobe, Japan.

7. RESPONSIBILITY NOTICE

The authors are the only responsible for the printed material included in this paper.